Chapter 5

Seam Effect of Wire-Grid Polarizer

To promote the efficiency of the polarizer in liquid crystal displays (LCDs), the other example of the extended planar optics, the wire-grid polarizer (WGP), will be discussed in this chapter with the focus on the seam effect between the WGP patches.

WGP is well known as a high efficient polarization beam splitter (PBS). Along with proper optical components, the WGP can perform high efficient polarization conversion.[1], [2] Compared with the conventional selective absorption polarizer in LCDs, a subwavelength grating module based on the WGP has demonstrated a factor of 1.7 enhancement in the polarization efficiency. [3],[4] However, to be operated in the visible spectrum, a WGP should possess a grating period of less than 150 nm to maintain the high transmission and reflection extinction ratios in the blue wavelength region.[5] Then, the WGP requires high-resolution techniques such as E-beam lithography to fabricate the sub-150-nm structures, and the mass production of such WGP becomes costly and time consuming. Although the cost-effective nano-imprint technique was exploited to fabricate a 5.5 x 5.5 cm^2 WGP with the period of 100 nm and a 4-in-diameter WGP with the period of 200 nm,[5], [6] for the large size display such as monitors, the reported sizes of WGPs remain insufficient and the “patching” technique becomes necessary.

As an efficient PBS, an ideal WGP device shall well separate the p-ray and s-ray. However, when a seam between the WGP patches exists, it allows both p-ray and s-ray to transmit with large portion, thus decreasing the polarization efficiency. By means of conventional techniques, the patched WGP can be realized using the step-and-repeat machine with a seam width around hundreds of micron. Since the

seams are inevitable for the patched WGP, it is essential to model the effect of seam before the WGP fabrication.

Various methods based on different theories, such as effective media theory and rigorous diffraction grating theory, have been applied to model the ideal one-patch WGP.[2],[7]-[10] Among these methods, the rigorous coupled-wave analysis method (RCWA) has been developed as a commercial software GSOLVER by which the simulations have shown good agreements with the experiments.[2],[3] Therefore, the RCWA method and GSOLVER are utilized herein to analyze the effects of the seams resulting from WGP patches, called the seam effect herein. Although the RCWA is an exact solution of Maxwell's equations and is widely used to analyze the electromagnetic diffraction,[11]-[12] the issues, such as poor convergence, were challenged in the previous literature.[7] In order to apply the RCWA effectively and numerically to the seam effect study, the critical issues are first discussed in this chapter, followed by the proposed strategy. Finally, the seam effect of a 100-nm-period WGP is analyzed as an example to obtain the design rules of WGP patching.

5.1 Investigation of seam effect by using RCWA

5.1.1 Review of literature

Moharam et al. have proposed efficient approaches to implement the RCWA of conventional one-patch gratings stably and mentioned that the two criteria for the numerical RCWA of conventional gratings were the energy conservation (diffraction efficiency DE ≤ 1) and the convergence with an increasing number of field harmonics (calculated diffraction orders).[11] To meliorate the numerical stability, they presented a method comprising formulation and normalization to preempt the numerical overflows and underflows. However, when boundary conditions were substituted into

the characteristic matrix, numerical truncations occurred. Along with the inversion calculation during the process of solving matrixes, such truncations might incur numerical errors and violate the rule of energy conservation.

5.1.2 Energy conservation

When the RCWA is applied to simulate the seam effect of WGP, the energy conservation becomes a serious issue. The reason can be interpreted as follows, and formulas derived from Moharam's research are referred to herein in order to simplify and clarify the explanation.[11] Consider that a plane wave with the wavelength λ_0 is obliquely incident from the medium I (refractive index = n_I) to a WGP with an angle of θ, as shown in Fig. 5-1. The period and thickness of grating are assumed as Λ and d, respectively.

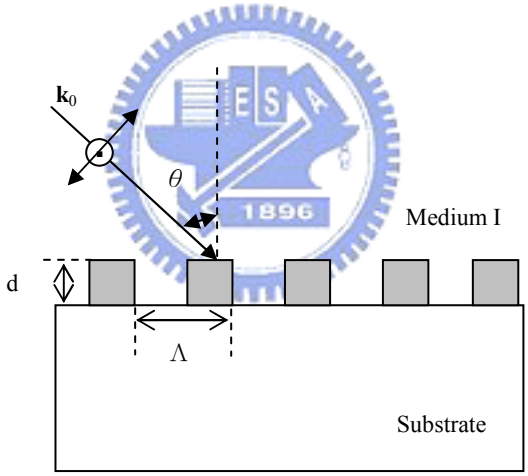

Fig. 5-1 Side view of wire-grid polarizer.

The permittivity of the grating can be expressed as a Fourier expansion:

$$\varepsilon(x) = \sum_h \varepsilon_h \exp(\, j2\pi h / \Lambda) \,. \tag{5-1}$$

Here, ε_h is the hth Fourier coefficient of the relative permittivity and can be derived from the grating structure. Then, when the incident light interacts with the WGP, the incident electric field E_0, also analyzed as Fourier harmonics, will be modulated by the grating. For simplicity, the transmission of WGP is considered herein instead of

both the transmission and the reflection. The transmitted coefficient of the *i*th harmonic, t_i, is defined as the *i*th harmonic of transmitted electric field Et_i over the incident electric field E_0. Assume that the permittivity and the electric field are both interpreted as Fourier harmonics with *r* orders for the numerical calculation. Through a series of matrix calculation to solve Maxwell's equation,[11] the coupled-wave phenomena then can be represented as a characteristic matrix **[A]**:

$$\mathbf{[A] = [N^2]-[E],} \tag{5-2}$$

where **[N]** is a diagonal matrix determined from the Floquet equation with the *i*, *i* element given by:

$$n_{i,i} = n_I \sin\theta - i\frac{\lambda_0}{\Lambda}, \qquad i = 1,\ 2,\ 3\ldots r \tag{5-3}$$

and **[E]** is the permittivity matrix with the *i*, *p* element given by $\varepsilon_{(i-p)}$. As a result, the *i*th transmitted coefficient t_i can be derived:[11]

$$t_i = \sum_{m=1}^{r} a_{i,m}^{+} \exp(-k_0 q_m d) - a_{i,m}^{-}, \tag{5-4}$$

where $k_0 = 2\pi/\lambda_0$ and q_m are the positive square roots of the eigen-values of **[A]**. $a_{i,m}^{+}$ and $a_{i,m}^{-}$ are the coefficients for the forward and the backward waves, respectively, derived from the boundary conditions and the coupled-wave matrix **[A]**. It is noted that since the assumed number of orders is *r*, **[A]**, **[N]** and **[E]** are all $r \times r$ square matrices.

To solve t_i via numerical methods, the inversion of $\exp(-k_0 q_m d)$ is inevitable. If $q_m d$ is a large positive value, then the computational truncation may cause the $\exp(-k_0 q_m d)$ to approach zero. Consequently, the inversion of exponent will be

$$\left(\exp(-k_0 q_m d)\right)^{-1} \sim (0)^{-1}, \tag{5-5}$$

which results in the truncation error. Therefore, those parameters incurring large $q_m d$ are the key factors that result in the energy conservation invalidated. Among the key factors, the number of orders (*r)* is investigated herein owing to its close relationship with the numerical accuracy, which will be discussed in next section. According to eq. (5-3), the upper limit of i and the maximum amplitude of $n_{i,i}$ will increase with r . Since q_m is derived from eq. (5-2), the probability of large positive q_m will also raise with the increasing r. Then, based on eq. (5-5), more truncation errors occur and the probability of the invalidation of energy conservation will increase. In other words, as the number of orders increases, the probability of the invalidation of energy conservation will also raise.

5.1.3 Numerical Accuracy

Although decreasing the number of calculated diffraction orders can reduce the probability of the invalidation of energy conservation, insufficient orders will cause poor convergence and inaccurate results in the analyses.[12] Therefore, we investigate the relationship between the number of orders and the accuracy in order to determine an adequate number of orders. Assume the width of each WGP patch (patch period), the period of gratings, the width of seam and the number of gratings per patch are denoted as P_p, P_g, W_s and g, respectively. As illustrated in Fig. 5-2, the patch period can be represented as:

$$P_p = g \cdot P_g + W_s . \tag{5-6}$$

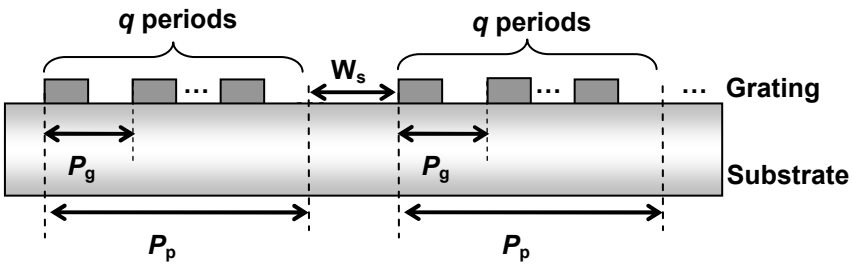

Fig. 5-2 Illustration of WGP patches.

Then the differential efficiencies (DEs) can be obtained by the substitution of P_p for the grating period in the conventional RCWA tool. It is noted that the simulated DE is regarded as converged and accurate only when the number of orders (*r)* exceeds a certain amount so that the resultant DE is a constant value. In the preliminary analysis, W_s is set to be zero and P_g is a constant. Then, since there is no seam between gratings in this analysis, different settings of g (the number of gratings per patch) represent an identical structure and the simulated results shall be the same. However, the modeling results in Fig. 5-3 show that the curve of efficiency versus r is horizontally expanded as g increases. Such horizontal-scaled curves result from the definition of "period". For the conventional RCWA tool which concerns gratings without seams, only one period (P_g) exists in the grating structure; the diffraction characteristics, such as diffraction angles and diffraction orders, are counted based on P_g. However, when patched gratings with seams are considered, there are two periods, P_g and P_p, in one device. In order to apply the tool to the patched gratings, the period parameter in the tool shall be set as the larger period which is P_p. As a result, the resultant diffraction characteristics are counted from P_p, which is a function of g. Thus, although the WGPs have the identical structure (due to the constant P_g and the zero W_s), the DE curves differ with the various g. Meanwhile, eq. (5-6) reveals that P_p in this preliminary analysis is in proportion to g and P_g, also explaining the effect of curve-scaling.

According to the mentioned curve-scaling effect, when the RCWA tool is utilized to analyze seam effect, the required number of orders shall be at the level in proportion to g for reasonable DE results. Therefore, if one patch comprises only one grating period, and its sufficient number of orders for accurate analyses is r_1, then for the case of one patch with g grating periods, the required number of orders r_g will be:

$$r_g = g \cdot r_1 . \tag{5-7}$$

As for the cases of $W_s \geq 0$, the number of orders shall be at least at the level of r_g to maintain the numerical accuracy.

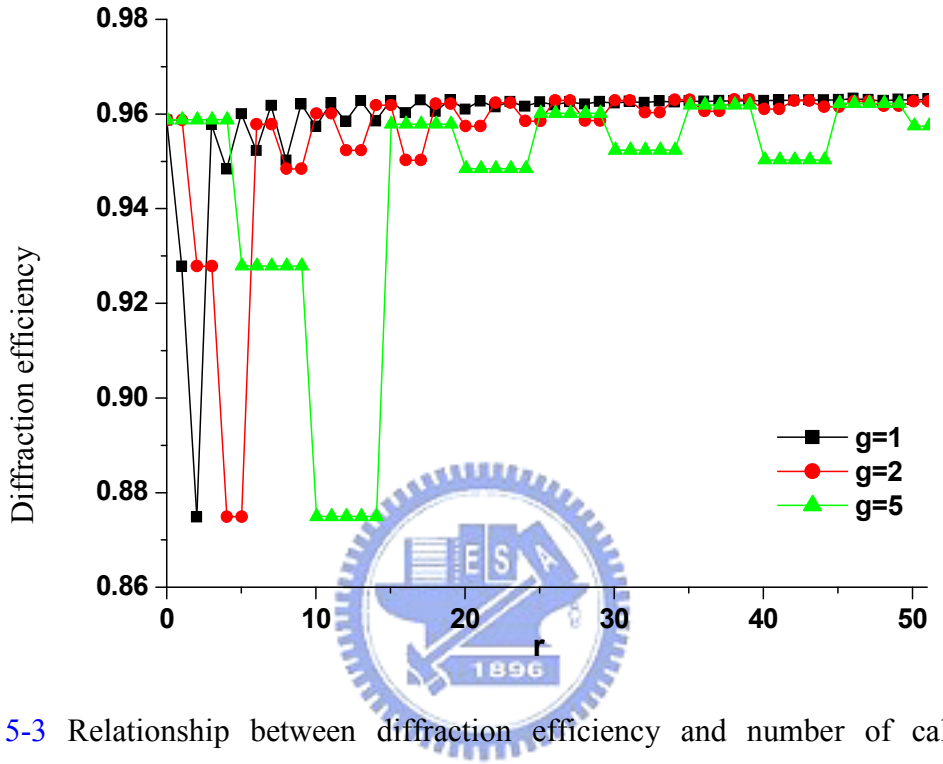

Fig. 5-3 Relationship between diffraction efficiency and number of calculated diffraction orders (r) for different numbers of gratings per patch (g=1, 2, 5).

Since energy conservation and numerical accuracy are closely related to the number of orders (r), a feasible strategy to determine r is proposed as follows. First, assume W_s and g to be zero and unity, respectively. Then, compute DE by increasing r_1 till the convergence occurs. Once r_1 is found sufficient for the convergence, the required level of r_g can be determined using eq. (5-7); then, the numerical accuracy is kept. Next, calculate the real case of WGP with the real W_s and g. If the resultant DE contradicts the rule of energy conservation (DE $\geq$ 1), adjust r_g by several increments till the rule of energy conservation is satisfied. Finally, the acquired DE can attain the accuracy requirement and be consistent with the energy conservation rule.

5.2 Analyses of WGP patches

5.2.1 Wide-seam WGP

In accordance with the above discussions, the proposed strategy is adopted for the following analyses of WGP patches. In the cases of a wide seam-width (that is, one more than 10 times of the wavelength), a large memory capacity is required for the RCWA of the whole WGP. On the contrary, geometric optics approximation can analyze such a wide seam efficiently. Therefore, for the WGP with a wide seam width, we propose a hybrid method which counts the diffraction efficiency in the sub-wavelength gratings region using the RCWA and that in the seam region using the geometric optics analysis.

Consider that a WGP has periodic patches with a constant seam width. Assume that the transmittance of p-ray and s-ray of the whole WGP are T_p and T_s, respectively, whereas those in the grating and seam regions are labeled as T_{pg}, T_{sg}, T_{ps}, and T_{ss}, respectively. Due to the wide-seam assumption, the seam width (W_s) and the width of grating region (P_p- W_s), as shown in Fig. 5-4, belong to the range where the geometric optics is effective.

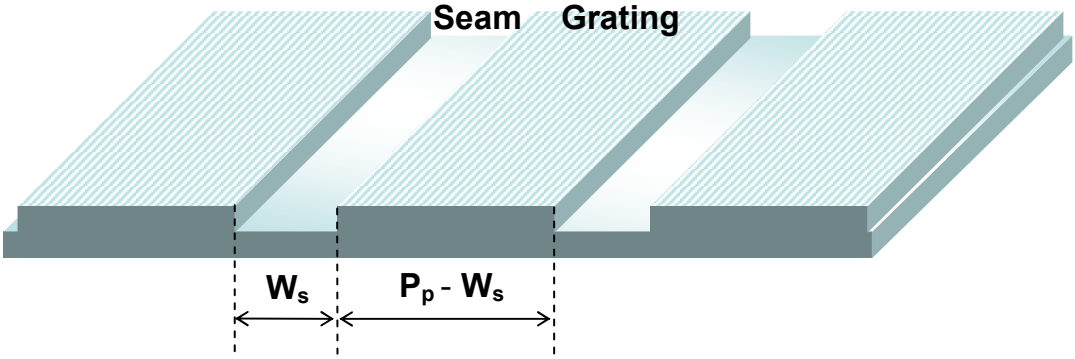

Fig. 5-4 Illustration of seam and grating regions.

Then the contribution of each region to the total transmission shall relate to their geometric portions, equivalent to the ratio of each width to the patch period:

$$T_p = \frac{T_{pg} \cdot (P_p - W_s) + T_{ps} \cdot W_s}{P_p}, \tag{5-8}$$

$$T_s = \frac{T_{sg} \cdot (P_p - W_s) + T_{ss} \cdot W_s}{P_p}. \tag{5-9}$$

As a result, an evaluated factor of transmission extinction ratio *EXT*, defined as T_p / T_s, is:

$$EXT = \frac{T_p}{T_s} = \frac{T_{pg} \cdot (P_p - W_s) + T_{ps} W_s}{T_{sg} \cdot (P_p - W_s) + T_{ss} W_s}. \tag{5-10}$$

In the grating region, regarded as ideal gratings without seam, T_{pg} and T_{sg} can be calculated using the numerical RCWA method with the setting of $W_s = 0$. Assume that a WGP consisting of a glass substrate and aluminum gratings is operated at the wavelength of 450 nm. The grating period, the grating height and the duty ratio are assigned as 100 nm, 140 nm and 0.5, respectively. The calculated T_{pg} and T_{sg} are 0.97 and 3 x 10^{-5}, respectively. In the seam region, due to the reflections between glass-air interfaces (3% for each interface), the transmission is assumed as 94% for both p-ray and s-ray. The relationship between *EXT* and W_s / P_p is then obtained, as solid line shown in Fig. 5-5. The results show that the lower ratio of seam width to patch period brings the higher extinction ratio. This curve also indicates that if the extinction ratio of 10 is required, the seam width should be of less than one-tenth of the patch period.

5.2.2 Narrow-seam WGP

On the other hand, for a WGP with a subwavelength seam width (that is, one ranging from $<< \lambda$ to $\sim \lambda$) the RCWA method alone is able to estimate the efficiency of WGP. Recently, using the commercial embossing machine with a state-of-art step-and-repeat machine, a WGP with nano-scale seam width of 100 nm has been

realized.[13] That is, the seam width of a WGP can be as narrow as 100 nm and, thus, can be analyzed by the RCWA method. Assume the condition is the same as the case of wide seam except for W_s = 100 nm. As the line with squares plotted in Fig. 5-5, the calculated results predict that W_s / P_p < 0.1 can lead to an *EXT* of more than 50. Compared with the wide seam case, the nano-seam WGP results in more enhancement of *EXT*. It is noticed that as W_s / P_p in the nano-seam case decreases, equivalent to an increase of the grating number per patch (due to the fixed P_g and W_s), the required computational memory will increase. Since the capacity of available memory is restricted by the computation system, the computable W_s / P_p is confronted with a lower limit which is 0.01 in our demonstration. To estimate a nano-seam WGP with further lower W_s / P_p, curve fitting is recommended to predict the tendency of *EXT*. According to the fitting results of this example, the *EXT* can exceed 1000 when W_s / P_p is lower than 0.001.

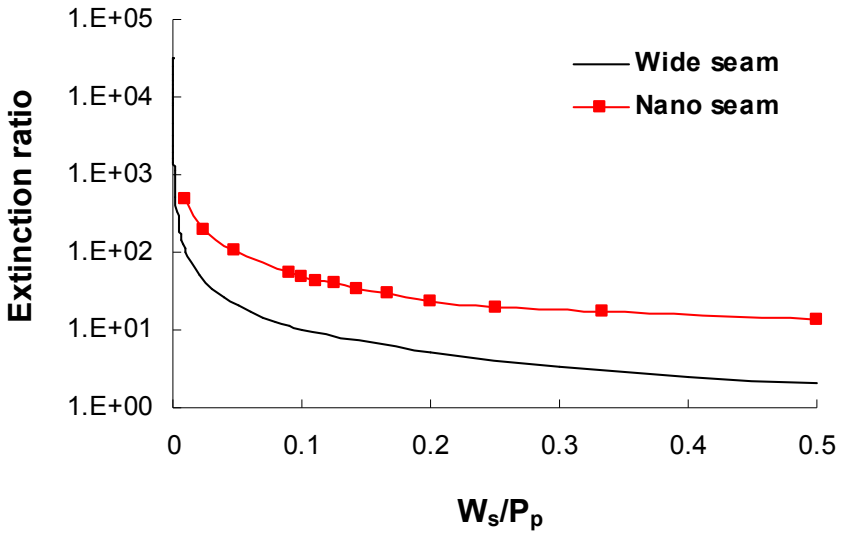

Fig. 5-5 Relationship between extinction ratio *Ws/Pp* for a wide-seam WGP (*Ws* >> λ) and a narrow-seam WGP (*Ws* = 100 nm).

5.2.3 Discussion

Although a finite-difference time-domain (FDTD) based method was used to model WGP,[14] the RCWA exhibits better simulation performance than the FDTD, as our numerical analysis shown in Table 5.1. Since the FDTD algorism implements the structure of device as spatial grids and the electromagnetic waves as temporal grids, its numerical accuracy dependents on the sufficiently small grids. Then, the larger simulated area requires the large memory capacity and the long simulation time. Thus, for the analyses of patched WGPs (with seams), the required simulation area shall be extensive, and the demand on memory capacity in the FDTD algorism becomes more serious. In contrast, the RCWA, using Fourier expansion to describe the structure of device, is adequate to model the periodic structure, such as the ideal one-patch WGP. As for analyzing WGP patches, the proposed strategies can allow the RCWA to model the seam effect with good modeling accuracy and efficient simulation speed. Therefore, the RCWA with the proposed strategies is preferable for modeling the WGP patches.

Table 5.1 Comparison of RCWA and FDTD for ideal WGP

Algorism	Software	Settings	Required memory	Execution time (s)
FDTD	Limerical FDTD Solutions	Simulation distance:100λ Grid: 5 nm x 5 nm Area: 10λ x 10λ	32Mbyte	255
RCWA	GSOLVER 4.20C	51 orders	23Mbyte	10
Common conditions	Wavelength: 450nm WGP: Glass substrate and Aluminum gratings with 100nm period, 140nm thickness and 50% duty cycle. Computer: Pentium 4 3.2GHz CPU and 504MB RAM			

Besides DE, the diffraction angle of the patched WGPs is another consideration of the seam effect. Assume that the patch size is fixed for every patch (patch period = P_p). According to the diffraction formula, ideal WGPs (with sub-wavelength gratings but without seam) allow only the zero-order diffraction to exist (the diffraction angle θ_d = 0° for the normal incident light). However, for a patched WGP, the periodic patches cause high-order diffractions to exist and the diffraction angle deviation becomes serious as P_p is reduced, as shown in Fig. 5-6 which considers the 1st order diffraction and normal incident light. The results reveal that for a WGP with a patch period of 10^5 times larger than the wavelength,[5],[6] the diffraction angle is controlled within $5.7\text{x}10^{-4}$ °, inferring insignificant deviation from the ideal case. Therefore, using currently available fabrication processes, the deviation of diffraction angle caused by the patched WGP shall be accepted.

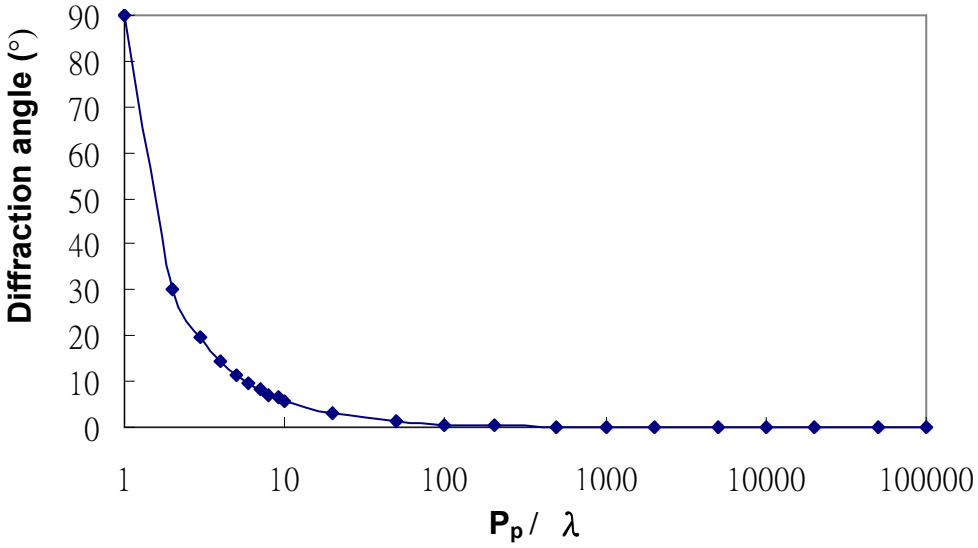

Fig. 5-6 Relationship between the 1st order diffraction angle and *Pp*/ λ.

5.3 Summary

The RCWA method was used to analyze the effects of the seams resulting from WGP patches. Within this framework, the modeling criteria of energy conservation and numerical accuracy were investigated and proved to be closely related to the number of calculated diffraction orders. With the strategies demonstrated in this research, the diffraction efficiencies satisfied the two criteria simultaneously, and then the widely used RCWA software, GSOLVER, was enabled to efficiently analyze the seam effect of the WGP patches. According to the numerical analyses, for a 100-nm-period WGP operated at a wavelength of 450 nm with the seam width of less than one-thousandth of the patch period, an extinction ratio of more than 1000 can be expected. In addition, the RCWA with proposed strategies was shown to be preferable for modeling the WGP patches due to its superior simulation speed. Consequently, this study presented a useful model for optimizing the nano-structured WGP design.

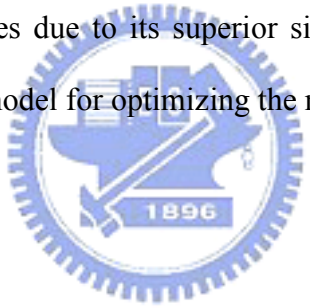

5.4 Reference

[1] J. Grinberg, and M. Little, U.S. Patent No. 4,688,897 (1987).

[2] X. Mi, D. Kessler, L. Tutt, L. Weller-Brophy, *2005 SID International Symposium Digest of Technical Papers*, pp. 1004-1007.

[3] KW. Chien and HP. D. Shieh, Appl. Opt. **43**, 1830-1834 (2004).

[4] KW. Chien and HP. D. Shieh, *2002SID International Symposium Digest of Technical Papers*, pp. 1229-1231.

[5] S. W. Ahn, K. D. Lee, J. S. Kim, S. H. Kim, J. D. Park, S. H. Lee and P. W. Yoon, Nanotechnology **16**, 1874–1877 (2005).

[6] J. J. Wang, J. Deng, X. Deng, F. Liu, P. Sciortino, L. Chen, A. Nikolov, and A. Graham, IEEE J. Sel. Top. Quant. **11**, 251-253 (2005).

[7] X. Yu and H. Kwok, J. Appl. Phys. **93**, 4407-4412 (2003).

[8] M. Paukshto, K. Lovetsky, A. Zhukov, V. Smirnov, D. Kibalov, and G. King, *2006 SID* International *Symposium Digest of Technical Papers*, pp. 848-850.

[9] X. Yu and H. Kwok, *2003 SID International Symposium Digest of Technical Papers*, pp. 878-881.

[10] T. Sergan, M. Lavrentovich, J. Kelly, E. Gardner, D. Hansen, J. Opt. Soc. Am. A, **19**, 1872-1885 (2002).

[11] M. G. Moharam, E. B. Grann, and D. A. Pommet, J. Opt. Soc. Am. A **12**, 1068-1076 (1995).

[12] M. G. Moharam, D. A. Pommet, and E. B. Grann, J. Opt. Soc. Am. A **12**, 1077-1086 (1995).

[13] G. Lecarpentier, *Short Course B of Symposium on Nano Device Technology 2006*, (National Nano Device Laboratories, Hsinchu, Taiwan, 2006), pp. 55-86.

[14] http://www.lumerical.com/fdtd.